

Article

Antimicrobial Properties of Polyester/Copper Nanocomposites by Melt-Spinning and Melt-Blowing Techniques

Alain González-Sánchez¹, Ricardo Rosas-Macías¹, José E. Hernández-Bautista¹, Janett A. Valdez-Garza¹, Nayeli Rodríguez-Fuentes² , Florentino Soriano-Corral³ , Antonio S. Ledezma-Pérez¹ , Carlos A. Ávila-Orta^{1,*}  and Víctor J. Cruz-Delgado^{3,*} 

- ¹ Departamento de Materiales Avanzados, Centro de Investigación en Química Aplicada, Saltillo 25294, CH, Mexico; alain.glez.sse@gmail.com (A.G.-S.); ricardo.rosmac@gmail.com (R.R.-M.); eduardo.hernandezbta@gmail.com (J.E.H.-B.); janett.valdez@ciqa.edu.mx (J.A.V.-G.); antonio.ledezma@ciqa.edu.mx (A.S.L.-P.)
- ² CONAHCYT—Unidad de Materiales, Centro de Investigación Científica de Yucatán, A.C, Mérida 97205, YU, Mexico; nayeli.rodriguez@cicy.mx
- ³ Departamento de Procesos de Transformación, Centro de Investigación en Química Aplicada, Saltillo 25294, CH, Mexico; florentino.soriano@ciqa.edu.mx
- * Correspondence: carlos.avila@ciqa.edu.mx (C.A.Á.-O.); victor.cruz@ciqa.edu.mx (V.J.C.-D.); Tel.: +52-844-4983890 (ext. 1391) (C.A.Á.-O.)

Abstract: In this study, textile fiber prototypes based on polyester and different Cu nanoparticles (CuNP) content were produced using melt-spinning to obtain bi-component multifilament fibers and melt-blowing to obtain non-woven fabrics. The prototypes were tested against pathogenic microorganisms such as *S. aureus*, *E. coli*, and *C. albicans*. It was shown that bi-component fibers offer excellent protection against pathogens, with up to 99% growth inhibition with 0.5% *w/w* for *S. aureus* and *E. coli*; meanwhile, non-woven fabric only shows activity against *E. coli* from 0.1% *w/w* of CuNP. Using different analytical techniques, it was possible to identify that the CuNP were confined exclusively in the outer cover of the bi-component fibers which may be associated with increased antimicrobial activity compared to the fibers in the non-woven fabric. The use of polymeric nanocomposites based on polyester/copper offers an alternative of great interest due to the versatility of the raw material and the high efficiency of copper nanoparticles as an antimicrobial additive.

Keywords: antimicrobial properties; nanocomposites; copper nanoparticles; melt-blowing; melt-spinning; textiles



Citation: González-Sánchez, A.; Rosas-Macías, R.; Hernández-Bautista, J.E.; Valdez-Garza, J.A.; Rodríguez-Fuentes, N.; Soriano-Corral, F.; Ledezma-Pérez, A.S.; Ávila-Orta, C.A.; Cruz-Delgado, V.J. Antimicrobial Properties of Polyester/Copper Nanocomposites by Melt-Spinning and Melt-Blowing Techniques. *Textiles* **2024**, *4*, 1–16. <https://doi.org/10.3390/textiles4010001>

Academic Editors: Selestina Gorgieva and Andrea Zille

Received: 30 October 2023

Revised: 2 December 2023

Accepted: 14 December 2023

Published: 25 December 2023



Copyright: © 2023 by the authors. Licensee MDPI, Basel, Switzerland. This article is an open access article distributed under the terms and conditions of the Creative Commons Attribution (CC BY) license (<https://creativecommons.org/licenses/by/4.0/>).

1. Introduction

Hospital-acquired infections (HAIs) have a tremendous economic and social impact nowadays due to loss of jobs and their elevated costs for health care. In 2016, USD 7.2 to 14.9 billion were spent on HAIs in the United States. Surgical site infections and infections with *Clostridioides difficile* accounted for 79% of the cost of HAIs [1]. The main microorganisms associated with HAIs are *Escherichia coli*, *Staphylococcus aureus*, *Enterococcus* spp., *Pseudomonas aeruginosa*, *Klebsiella* spp., and *Clostridioides difficile*, among others. Meanwhile, their prevalence over time remains almost constant [2]. Sanitization of medical personnel is one of the main strategies to reduce the incidence of HAIs. Another strategy is to provide effective and low-cost barriers that prevent the proliferation of pathogenic microorganisms in hospital environments, such as in coatings for walls, equipment surfaces, and clothing [3]. Reusable and disposable textile clothing is the front barrier for medical personnel, where the incorporation of antimicrobial agents hinders the accumulation of pathogenic microorganisms, resulting in antimicrobial textiles.

Tanasa et al. have identified four large groups of antimicrobial textiles. They were identified as textiles with (i) antimicrobial functionality, (ii) antimicrobial polysaccharides,

(iii) antimicrobial metallic nanoparticles, and (iv) antimicrobial synthetic compounds [4]. However, considering their antimicrobial effectiveness and mechanisms of action, as well as their toxicity versus tolerance, textiles with antimicrobial functionality can be divided into several classes [5]: (i) biostats, biocides (antibacterial, antifungal, antiviral), barriers, and antibiofilm; (ii) textiles with bound or leaching antimicrobial finishing; (iii) textiles made of natural or synthetic fibers or blends; (iv) textiles able to release compounds with biological activity; and (v) wearables and washing-resistant textiles.

Of particular interest is the use of antimicrobial metallic nanoparticles such as silver (AgNP), gold (AuNP), copper (CuNP), zinc (ZnNP), titanium (TiNP), and its oxides, as well as graphene to combat most common and proliferating pathogens in hospital environments resulting in HAIs. These nanoparticles stand out due to the high levels of effectiveness shown even at very low concentrations [6–12]. Metallic nanoparticles can be incorporated or impregnated into fibers (either filaments of non-woven fabrics) to produce antimicrobial fibers. Textile filaments from synthetic polymers such as polyester (usually polyethylene terephthalate, PET) can be produced industrially through melt-spinning, while non-woven fabrics (NWFs) of the same can be fabricated by means of melt-blowing. It is well-known that other processes can result in filaments and NWF, but they are outside of the scope of this study.

With the growing demand for personal protective equipment (PPE) in the face of the pandemic events caused by SARS-CoV-2, the opportunity arises to develop materials with characteristics such as antimicrobial, antiviral, antifungal activity, etc. Zhou et al. used a kind of Cu_2O and $\text{Cu}_2\text{O@ZrP}$ micro-nanocomposite by loading Cu_2O onto ZrP nanoflakes through an in situ polymerization method, and $\text{Cu}_2\text{O@ZrP}$ composite could be successfully and uniformly integrated into PET fibers, presenting highly enhanced mechanical properties and antibacterial activities against *E. coli*, *S. aureus*, and *C. albicans* compared to its control sample obtained by the melt-blending method. In addition, the dispersion of nano- $\text{Cu}_2\text{O@ZrP}$ in the corresponding fabricated PET matrix was also compared and discussed in detail. The integration of Cu_2O and its nanohybrids through the in situ polymerization method yields high antibacterial activity at low contents such as 0.2 and 0.4% *w/w*. As is well known, Cu oxides possess higher antibacterial activity than their metallic counterparts. In addition, the integration within the layered structure of ZrP enhances the dispersibility in the fibers obtained [13].

Zhu et al. prepared an antimicrobial PET masterbatch using a magnesium-based antimicrobial agent (MAA, MgO) as the functional material by melt-blending. A kind of antimicrobial fabric was prepared using PET masterbatch and pure PET resin by high-speed melt-spinning and weaving technology with contents of 1, 2, 3, 4, and 5% *w/w* of MAA. A series of techniques was used to characterize the fibers and fabrics, and the antimicrobial property of the fabrics was tested against *E. coli*, *S. aureus*, *C. albicans*, and *A. niger* using the alive-microorganisms-counting method. Additionally, the physico-mechanical properties of fabrics were also tested, and the antimicrobial properties, after washing, were found to diminish very slowly after 50 cycles [14].

Yeo and Jeong prepared continuous bi-component core-shell fibers using a melt-spinning method with polypropylene and silver nanoparticles. The melt-spun fibers were characterized using different techniques. The antibacterial effect was evaluated by the AATCC 100 test. The DSC thermograms and X-ray diffraction intensity pattern results indicated that the crystallinity of polypropylene, including silver nanoparticles, decreased slightly compared with that of pure polypropylene fibers. SEM micrographs showed that the average diameter of the silver nanoparticles was approximately 30 nm, and that some particles had aggregated. The fibers contained silver in the central part (core) and did not show antibacterial effects. However, the silver fibers added to the shell part showed excellent antibacterial effects against different bacteria using concentrations of 0.3 and 5% *w/w* [15].

Other studies have dealt with polymer fibers containing metal nanoparticles. However, the authors have focused on processability and physical properties rather than antimicro-

bial properties in these cases. Guerra et al. prepared potential antimicrobial PET-AgNP nanocomposite filaments for textile applications, incorporating AgNP in a PET matrix at different concentrations by extruding the PET resin with specific amounts of a 10% (*w/w*) AgNP/PET masterbatch. Then, rheological characterization was carried out, and filaments were produced for mechanical, optical, and thermal analyses. Incorporating up to 0.20% (*w/w*) of AgNP in the polymeric matrix did not significantly alter the overall properties of the PET nanocomposites. Beyond this quantity, the processability of the polymeric nanocomposite for forming filaments was compromised [16].

Meanwhile, Guzman et al. described the preparation and characterization of a bactericidal synthetic fiber composed of recycled polyethylene terephthalate (rPET) and CuNP through an extrusion process using triethylene glycol as a solvent, which allowed for mixture to be fluidized through the extruder. The degree of dispersion of the nanoparticles in the PET matrix was studied using X-ray diffraction and scanning electron microscopy. X-ray fluorescence was used to demonstrate the presence of copper in the polymer matrix of the fiber. At the same time, the mechanical properties of the obtained fiber were evaluated [17].

On the other hand, non-woven fabrics have found many applications due to their intrinsic properties like filtration, absorbency/repellent, antimicrobial/antiviral, lightweight, pore size control, and thermal/acoustic insulation, among others. However, some of these properties require additives, usually applied externally or on the finished product, to reduce the additive content use. The need to wear a face mask in public spaces was implemented during the 2019 coronavirus pandemic to lower infections between populations. Different approaches were tested to increase the effectiveness of these products from a scientific and industrial point of view.

One study by Abazari et al. aimed to impregnate the masks with silver nanoparticles through a sonochemical treatment. Therefore, the polypropylene NWF substrates were treated at different sonication times and AgNP concentrations. Different parameters, such as AgNP release, filtration efficiency, pressure drop, electrical conductivity, and antibacterial activity against *E. coli* and *S. aureus*, were evaluated in the treated masks. The results showed that by using longer sonication times and greater concentrations of the AgNP precursor a more significant and stable coating and higher antibacterial activity were obtained without sacrificing cytotoxicity towards *Artemia nauplii* cell lines. The above suggests its potential application for protection masks against different pathogenic entities [18]. In another work by Ferreira et al., different polypropylene NWFs were characterized by their structural, physicochemical, and comfort-related properties to obtain three-layer masks. The NWF selected for the interlayer was functionalized using three different methods with 0.3 and 1.2% *w/w* of zinc oxide nanoparticles (ZnO NPs). The functionalized fabrics obtained by dry pad immersion revealed the most promising data, with $0.017 \pm 0.013\%$ *w/w* ZnO NPs located mainly on the fiber surface and being capable of completely eradicating *S. aureus* and *E. coli* colonies within the 24 h tested (ISO 22196) in addition to contributing to the inhibition of the growth of a substitute for the SARS-CoV-2 virus (ISO 18184 standard). The developed three-layer, multi-scale fibrous structures with antimicrobial capabilities have immense potential as functional protective masks [19]. The applications of silver, copper, and zinc ions as well as metallic particles of Cu, Ti, and Zn oxides are useful antimicrobial reagents for the biofunctionalization of various materials and their surfaces. In this sense, aqueous dispersion of synthetic copolymers based on acrylics and the above-mentioned nanoparticles were used to modify the surface of NWFs of polyester and polylactic acid (PLA). The antimicrobial (antibacterial and antifungal) properties of the textile materials (fabrics and non-wovens) functionalized with the above-mentioned active agents exhibiting antimicrobial properties (CuSiO₃, TiO₂, ZnO, or ZnO·SiO₂) were highly dependent on the content of the agents in water dispersions. These new functionalized, non-woven polymeric textile materials can find practical applications in manufacturing filters for hospital air conditioning systems, the automotive industry, and air purification devices [20]. Gabbay et al. conferred that cotton and polyester fibers exhibit a broad spectrum of properties against bacteria, viruses, and fungus using impregnation or coating with cationic copper.

This platform allows for the mass production of woven and non-woven fabrics such as sheets, pillow covers, gowns, socks, and air filters, among others, without the need to alter any industrial procedures or machinery—only the introduction of copper oxide-treated fibers containing 3–10% *w/w*. These authors point out that impregnated fibers do not interfere with handling end products, washing cycles, color changes, press, etc. At the same time, antimicrobial fabrics can alleviate athletes' feet or decrease bacterial colonization in a clinical setting; additionally, they do not have skin sensitizing or adverse effects [21].

Comparison of the processing of polymeric nanocomposites with metallic nanoparticles using melt-spinning and melt-blowing techniques and the evaluation of their antimicrobial activity using the same nanocomposite and antimicrobial agent contents is important because these materials would not require a finishing treatment and have an inherent antimicrobial function. The relevance of this study lies in the feasibility of testing both processing methods and comparing the performance of the prototypes obtained against a series of microorganisms of clinical interest. Therefore, in the present study, the behavior of polymeric nanocomposites based on CuNP and polyester is studied to determine their viability of being converted into a textile using two different techniques, such as melt-spinning and melt-blowing. Furthermore, we aim to subsequently evaluate their structural, morphological, and antimicrobial properties against various pathogenic microorganisms, depending on the CuNP content and the method of obtaining the textile. The results will determine whether these textiles can be used to manufacture personal protective equipment that help mitigate the proliferation of pathogens for medical personnel, hospital textiles, and air filters, among others.

2. Materials and Methods

Commercial copper nanoparticles (CuNP) with a purity of 99.8%, an average diameter of 25 nm, and hemispherical geometry were used, according to data from the supplier SkySpring Nanomaterials (Houston, TX, USA). The polyethylene terephthalate resin (PET) used was provided by Indorama Ventures Inc. company (Queretaro, Mexico) and used in the injection molding process with an intrinsic viscosity (IV) of 0.82 ± 0.02 , melting temperature of 252 °C, and about 12% composition of solids. To avoid oxidation of CuNP, they were previously mixed with mineral oil in an inert nitrogen atmosphere and kept under mechanical stirring for 1 h. Subsequently, they were added to a determined amount of previously dried polyester resin and mixed uniformly to coat the resin pellets. This mixture of resin and CuNP was processed by melt-mixing to obtain a masterbatch with a concentration of 1% by weight, as described below.

Masterbatch preparation (PET/1% CuNP). To obtain a uniform dispersion of 1% *w/w* CuNP in the polyester resin, the ultrasound-assisted melt extrusion (USME) technique was used, for which a Thermo Scientific twin-screw extruder model Prism TSE 24-MC (Karlsruhe, Germany) was used, which had a screw diameter of 24 mm and an L/D ratio 40:1, with 2 intensive mixing zones. A flat temperature profile of 260 °C was used. An accessory was attached to the extruder die to apply ultrasound waves of variable frequency between 15 and 50 kHz, with a power of 750 W, as described previously [22]. The material processed this way was cooled, cut, and placed in an oven at 120 °C for 12 h to promote its recrystallization before being processed using melt-spinning and melt-blowing techniques.

Fibers preparation. The preparation of multifilament fibers and non-woven fabrics was carried out in a multi-functional laboratory in pilot melt-spinning systems from Fiber Extrusion Technology (Leeds, UK) using the FET-100 Extrusion, FET-101 Multifilament, and FET-102 Non-woven modules, which have two single-screw extruders with a screw diameter of 25 mm and 20 mm, respectively, both with an L/D ratio of 30:1.

Multifilaments by melt-spinning. In this case, the two extruders were used. The purpose of performing co-extrusion was to obtain a fiber with a core-shell configuration and expose the CuNP on the surface of the fiber. To achieve this objective, neat polyester resin was fed into one extruder to form the core, and the PET/1% CuNP masterbatch was fed into the other extruder and mixed with more polyester resin to dilute its concentration

until obtaining final concentrations of 0.1, 0.25, and 0.5% by weight directly during the extrusion process. In both extruders, a temperature of 295 °C was used throughout the barrel, dosing pump, head, and spinneret. The multifilaments obtained were cooled with air and subjected to stretching using three rollers operating at different temperatures (25, 90, and 110 °C) and speeds (100, 120, and 240 mpm), respectively. They were collected in the winder using a speed of 300 mpm to obtain a stretching ratio of 3:1. A circular spinneret with 18 holes with a diameter of 0.125 mm and a length of 1.4 mm was used.

Non-woven fabrics by melt-blowing. In this case, only the 25 mm extruder was used, where the PET/1% CuNP masterbatch was mixed with more polyester resin to dilute its concentration until obtaining final concentrations of 0.1, 0.25, and 0.5% *w/w* directly during the extrusion process. A temperature of 295 °C was used throughout the barrel, dosing pump, head, and spinneret. An airflow of 1000 L/min was used at 300 °C to stretch the filaments and form the non-woven fabric. The filaments were deposited on a conveyor belt advancing at a speed of 0.6 mpm and were finally collected in a winder on a cardboard core. A straight spinneret with 41 holes with a diameter of 0.250 mm and a length of 2.4 mm was used.

Characterization. Differential scanning calorimetry (DSC) was used to determine the main transition temperatures of the PET and PET/CuNP masterbatch. DSC Discovery Series 2500 equipment from TA Instruments (New Castle, DE, USA) and a heating/cooling rate of 10 °C/min in a range of 10–300 °C were used in addition to inert atmosphere with nitrogen gas with a flow of 50 mL/min.

Thermal stability of the material during the subsequent melt-spinning and melt-blowing processes was analyzed by a thermogravimetric analyzer (TGA) model Q500 from TA Instruments (New Castle, DE, USA); the analysis conditions were heating from 25 to 800 °C at a rate of 10 °C/min, a nitrogen flow of 50 mL/min, and use of approximately 8–10 mg of each sample.

The denier of the multifilaments was calculated according to the linear mass ratio (gr) of each 9000 m of fiber obtained in the melt-spinning process. Likewise, the density of the NWF was determined in 10 × 10 cm samples; in both cases, an OHAUS Explorer (Newark, NJ, USA) analytical balance was used with a resolution of 0.0001 g.

Samples obtained through the melt-spinning processes were observed through an Olympus BX53 optical microscope (Tokyo, Japan), which has a digital camera attached that allowed for the capture of images.

The chemical analysis and morphology observation of the samples was carried out using a field emission scanning electron microscope JEOL, model JSM-7401F (Tokyo, Japan). The operating conditions were 2.0 kV acceleration voltage and a working distance of 8 mm. The multifilament samples were previously cryo-fractured by introducing filaments in liquid nitrogen for about 10 min and then fractured with the aid of a couple of tweezers. For NWF, a sample of about 1 cm × 1 cm was cut with scissors at room temperature. Both samples were placed on a sample holder with double-sided adhesive tape and coated with gold-palladium by ion sputtering about 60 s before observation.

The evaluation of the antibacterial activity of the materials was made, taking the JIS Z2801 as reference [23]. The test was performed for two microorganisms of clinical importance, *Staphylococcus aureus* ATCC-29213 and *Escherichia coli* ATCC-25922. For the test, samples of 0.5 g under aseptic conditions were inoculated with 4 mL of a microorganism suspension in trypticase soy broth, equivalent to 50,000 colony forming units per mL (CFU/mL). Subsequently, the samples were incubated at a temperature of 37 °C and 90% humidity for 24 h. At the end of the incubation time the population of microorganisms present in the samples was determined (the tests were performed in triplicate) and the antibacterial activity (R) was calculated using Equation (1):

$$R = (\log B_t B_0 - \log M_t B_0) \quad (1)$$

where B₀ and B_t are the amounts in CFU/mL of bacteria that survive in the presence of the reference (material without antimicrobial agent) before and after 24 h of incubation,

respectively. M_t is the amount of bacteria that survive after 24 h of incubation in the presence of the antimicrobial material (material with antimicrobial agent). Additionally, the inhibition to bacterial growth (GI) was determined by means of Equation (2):

$$GI = (B_t - M_t B_t) \times 100 \quad (2)$$

In the case of non-woven fabrics, the agar diffusion tests were carried out using strains of *Staphylococcus aureus* (*S. aureus*), *Escherichia coli* (*E. coli*), and *Candida albicans* (*C. albicans*). During the procedure, the turbidity of the suspension was adjusted to the McFarland turbidity standard of 0.5. At this absorbance, the bacteria concentration was standardized to approximately 1.5×10^8 CFU/mL and was used as a working microbial solution to inoculate the culture medium. A portion of approximately 1×1 cm of the different samples was placed in the center of the culture medium. The JIS and agar diffusion standards specify the use of 2 reference microorganisms, like *S. aureus* and *E. coli*, as representative groups of Gram (+) and Gram (−) microorganisms, while *C. albicans* is considered a microorganism of great importance in the health sector.

Data were statistically analyzed using a one-way variance analysis (ANOVA) followed by Tuckey's test. The significance level was set at 5%, and OriginPro software (version 2021) was used for the analysis.

3. Results

3.1. Masterbatch Characterization

3.1.1. Differential Scanning Calorimetry (DSC)

It is known that with the incorporation of nanoparticles in thermoplastic polymers, the main thermal transitions (glass transition (T_g), melting (T_m), crystallization (T_c)) can show variations with respect to the neat polymer. The above must be considered when these nanocomposites are transformed into a final product. Using DSC, it was possible to determine the melting behavior during heating fusion for the PET and PET/1% CuNP samples which were used as a masterbatch to obtain lower concentrations by dilution. Firstly, it was observed that the PET sample had a T_g of around 78 °C and a melting temperature T_m of around 242 °C. In the case of the masterbatch, it exhibited a T_g of about 80 °C, as well as a small endothermic transition around 138 °C (due to the mineral oil). In comparison, the melting temperature T_m increased to 250 °C, which indicates that the presence of CuNP shifted the melting of the material to higher temperatures (Figure 1A). The above may be due to the formation of crystals with greater perfection, which may have formed from CuNP that were homogeneously dispersed and acted as nucleation agents.

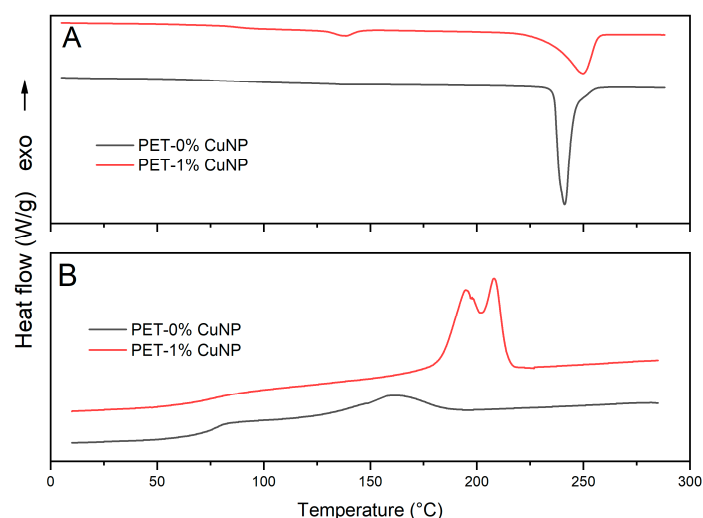


Figure 1. DSC thermograms for PET and PET/CuNP samples, at a heating/cooling rate of 10 °C/min and an inert atmosphere of N₂ gas with a flow of 50 mL/min. (A) Heating and (B) cooling.

During cooling (Figure 1B), it can be seen that the PET sample had a crystallization temperature T_c located at 152 °C and a T_g of around 80 °C, which corresponds well to a neat polyester resin that does not contain additives and/or copolymers that prevent or delay crystallization. For its part, the PET/1% CuNP sample exhibited a notable increase in the crystallization temperature, with a shift towards higher temperatures, in addition to the formation of two crystalline populations at 207 and 195 °C, respectively, as well as a T_g that was around 80 °C. The increase in T_c and the formation of two crystalline populations suggests, as indicated above, that CuNP are homogeneously dispersed in the PET matrix, acting as nucleation agents, generating more homogeneous crystals that crystallize at higher temperatures, in addition to the presence of secondary crystals that can originate at the expense of the first ones. On the other hand, this behavior during crystallization is typical in polyester resins in the presence of small amounts of nucleating agents. With the purpose of avoiding early solidification of the material in some areas of the extrusion process, the increase in crystallization temperature is a parameter that must be considered during the melt-spinning and melt-blowing processes which the material obtained will be subjected to.

3.1.2. Thermogravimetric Analysis (TGA)

A thermogravimetric study was carried out to demonstrate whether the presence of CuNP promotes an increase or decrease in the thermal stability of the masterbatch prior to being processed using melt-spinning and melt-blowing techniques. The results are shown in Figure 2. As the temperature increases, the PET sample presents a single weight loss event that begins around 380 °C and ends at approximately 460 °C. With the addition of 1% (*w/w*) CuNP, the sample also presents a single degradation event, which begins at slightly lower temperatures without evidencing any anomalous behavior. Based on this study, the polymeric nanocomposite can be considered thermally stable during the conditions required in melt-blowing and melt-spinning processes.

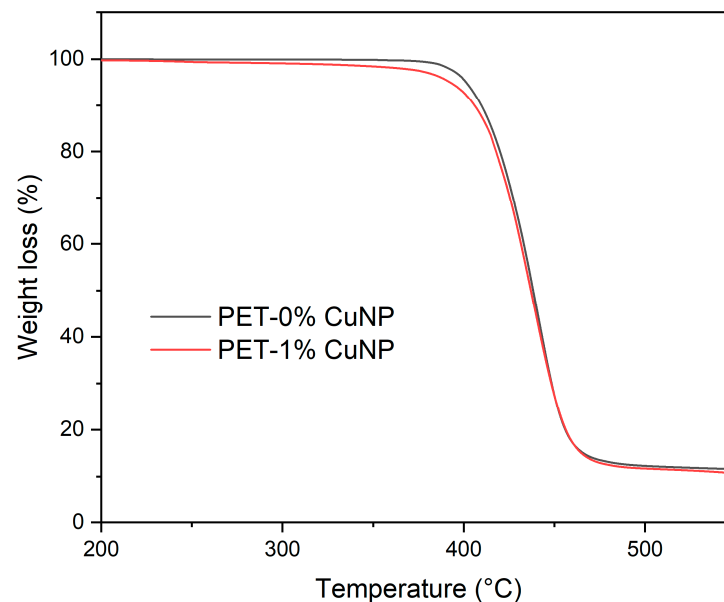


Figure 2. TGA thermograms for the PET and PET/CuNP samples at a heating rate of 10 °C/min and an inert atmosphere of N₂ gas with a flow of 50 mL/min.

Based on the previous results and taking into consideration that a dilution of the masterbatch will be carried out during the processing of the samples by melt-spinning and melt-blowing, the DSC and TGA techniques can be considered to provide sufficient information regarding the profile temperature that should be used for processing the samples. Although it is important to consider the flow properties of the polyester based on the shear speed and/or the determination of the fluidity index, it is widely known

that polyesters, polyamides, and other engineering polymers usually suffer a decrease in molecular weight after an extrusion cycle, which improves its fluidity and facilitates processing in a subsequent extrusion cycle.

3.2. Multifilament and NWF Characterization

Multifilament bi-component fibers produced by melt-spinning and NWF fabricated by means of melt-blowing were characterized by physical properties and morphology prior to their antimicrobial analysis.

3.2.1. Denier and Grammage

According to the total denier (TD) calculations corresponding to the lineal mass of 9000 m, expressed in g, a gradual increase in this parameter was observed as the Cu content increased, as shown in Table 1. Additionally, the denier per fiber (DPF) was calculated to obtain the individual linear mass of each fiber. The statistical analysis showed a significant difference between the weight of samples for TD and DFP. The latter would be associated with the quantity and density of copper, 8.96 g/cm^3 , which is 6 times higher than that of the polymer resin 1.39 g/cm^3 . On the other hand, the weight of the non-woven fabric was determined; this constitutes the weight per square meter, expressed as g/m^2 or gsm . This parameter is shown in Table 1 for the fabricated non-woven fabrics as a function of the concentration of CuNP. This value increased depending on the nanoparticle content. However, this increase did not show significant differences ($p < 0.05$) compared to the increase in denier.

Table 1. Denier in multifilament fibers and grammage in NWF with different CuNP content.

Sample	Multifilament		NWF Grammage
	TD	DFP	
PET/0.0% CuNP	222 ± 0.007^a	12.3 ± 0.000^a	67.5 ± 0.061^a
PET/0.10% CuNP	345 ± 0.005^b	19.1 ± 0.000^b	68.3 ± 0.041^a
PET/0.25% CuNP	369 ± 0.007^c	20.5 ± 0.000^c	68.8 ± 0.020^a
PET/0.50% CuNP	391 ± 0.009^d	21.7 ± 0.000^d	69.5 ± 0.078^a

Different lowercase letters in the same column indicate a significant difference ($p \leq 0.05$).

3.2.2. Multifilament Morphology

Fiber morphology. To demonstrate the formation of a core and shell in the bi-component multifilaments, several un-stretched filaments were placed in a sample holder, and a cross-section was made with the help of a sharp knife to avoid as much as possible deformation of the filament. The cut was carried out at room temperature, see Figure 3. As shown in Figure 3A, the cross-section of the filaments is circular. In this case, it is impossible to identify the border between the core and the shell because both sections are made of the same material, and there is no contrast between them. As the CuNP content increases, the formation of a halo or shell in each filament is observed, and this is better defined in Figure 3D, which corresponds to the highest CuNP content (0.5% w/w). It can also be seen that there is a heterogeneous distribution in the diameter of the filaments, which is more uniform in Figure 3D. According to the information collected through this technique, it was determined that the proportion of the core/shell was on average 80:20. The diameter of the filaments was $17 \pm 3 \mu\text{m}$, at a draw ratio of 3:1. It is considered that the proportion between the core/shell remains in a similar proportion after the drawing process, which would still confine more to the CuNP in the shell of each filament since their thickness decreases proportionally [24–27].

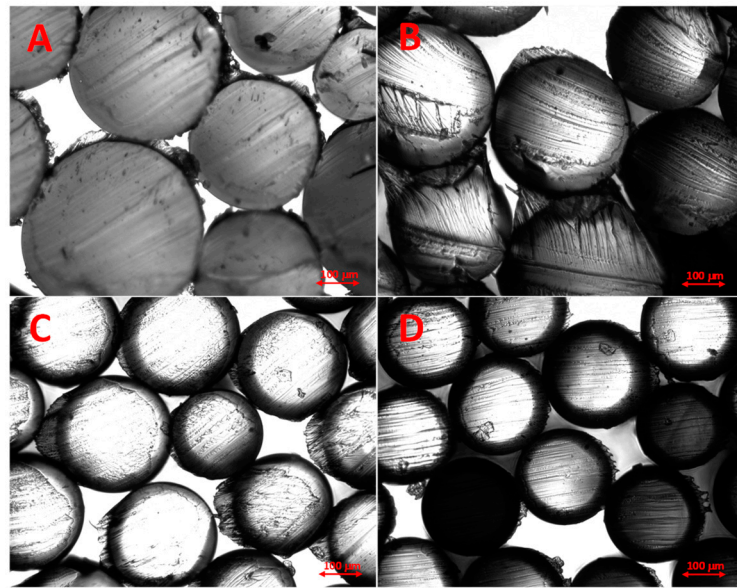


Figure 3. Optical microscopy images of filaments with core/shell configuration and different CuNP contents of (A) 0%, (B) 0.1%, (C) 0.25%, and (D) 0.5% at a magnification of 10 \times .

Morphology and elemental analysis by SEM. To corroborate the presence of CuNP in the bi-component multifilament, elemental analysis was performed on different sections of the shell filament by means of SEM, as seen in Figure 4. Once again, the image corroborates the circular shape of the filaments. Figure 4A corresponds to the PET sample; the cryo-fracture of the filament shows good compatibility between core and shell, and no contrast or evidence of the concentric fiber was observed. Meanwhile, for PET/CuNP at 0.5% *w/w* (Figure 4B), it is impossible to identify the core and shell zones due to the excellent compatibility of both samples. Elemental analysis was implemented in two specific zones near the surface of the filament, identified with the numbers 1 and 2 which correspond with the EDS analysis, as shown in Figure 4C. In both zones, a Cu signal appears, and this could be related to the confinement of the CuNP during the bi-component fiber forming, wherein the PET/CuNP nanocomposite was placed in the shell of the filament [24,26].

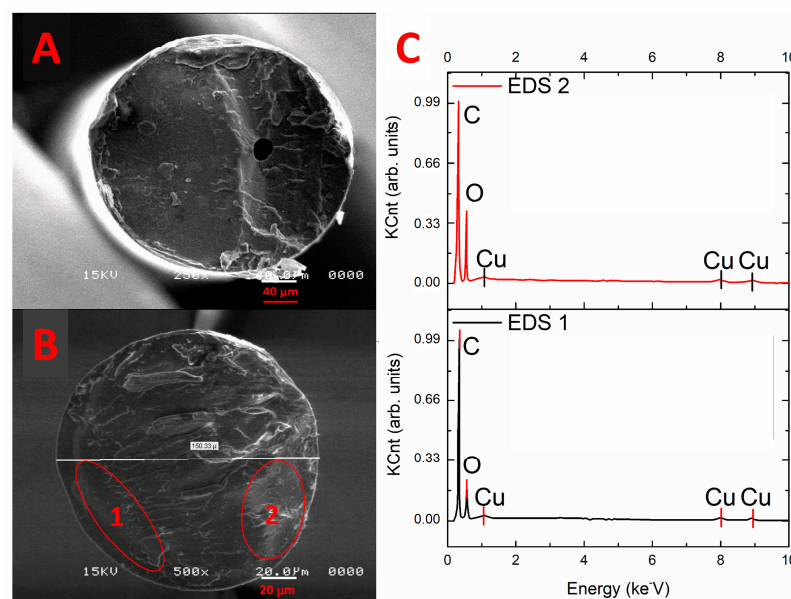


Figure 4. SEM image of the cryo-fractured cross-section filaments with core/shell configuration with (A) 0% *w/w* and (B) 0.5% *w/w* of CuNP, and (C) elemental analysis of sample B.

3.2.3. NWF Morphology

Morphology and elemental analysis by SEM. Figure 5 shows images corresponding to NWFs with 0.5% CuNP with different magnifications. As can be seen in greater detail in Figure 5A, the fibers have an average diameter distribution of 8 ± 4 microns, which suggests that the diameters are quite uniform. Furthermore, it can be seen that the fibers have a cylindrical structure apparently free of defects and do not resemble a union between them. In Figure 5B, the deposit of small particles of some contaminant, probably dust, with an average size between 1 and 3 microns can be seen, which should not be confused with CuNP, which have lengths less than 100 nm. In Figure 5C, observed at $10,000\times$, clear spots which are separated and distributed over the entire surface begin to be seen on the surface of the fiber, in addition to having sizes less than 1 micron, which are identified in the figure with a red circle. In Figure 5D, observed at $30,000\times$, white dots with a semi-circular geometry and sizes less than 100 nm can be seen, corresponding with the CuNP introduced into the fibers and exposed on the surface (identified with a series of circles). In addition, the appearance of a groove suggests the nanoparticle was dragged on the surface of the fiber, which could have happened during the stretching of the filaments when the sample was fabricated.



Figure 5. SEM images for the NWF of PET/CuNP (0.5% *w/w*) sample at different magnifications. (A) $350\times$, (B) $1000\times$, (C) $10,000\times$ and (D) $30,000\times$, and (E) elemental analysis of the sample.

An elemental analysis was carried out on this sample to corroborate the presence of copper in the fiber. In Figure 5E, it can be seen that, in addition to C and O, the other elements present are Cu and Ca, and Ca may have come from catalysts and/or additives used in polyester synthesis. Due to the NWF preparation method, we consider that not all the Cu was exposed on the surface of each fiber and that a large part of it was dispersed inside the fiber. The above may have considerable repercussions regarding the fabric's activity against different microorganisms.

3.2.4. Antimicrobial Properties

Multifilaments. Figure 6 shows the results obtained for the inhibition of the growth of bacteria *E. coli* (Gram-negative) and *S. aureus* (Gram-positive) following the procedure described in [23] and reported in previous work [28]. The antimicrobial activity, indicated as a percentage of inhibition, shows an increase in the ability of the multifilaments with different concentrations of CuNP to inhibit the growth of bacteria in both cases as the content increases, too. It should be noted that *E. coli* turned out to be more susceptible to CuNP from a concentration of 0.25%, showing a reduction of 90% and close to 99% in the growth of the microorganism with a 0.5% (*w/w*) CuNP content. For its part, *S. aureus* presents more excellent resistance when using concentrations of less than 0.25% of CuNP; while with 0.5%, the inhibition percentage is close to 100% with a content 5.0×10^4 CFU/mL.

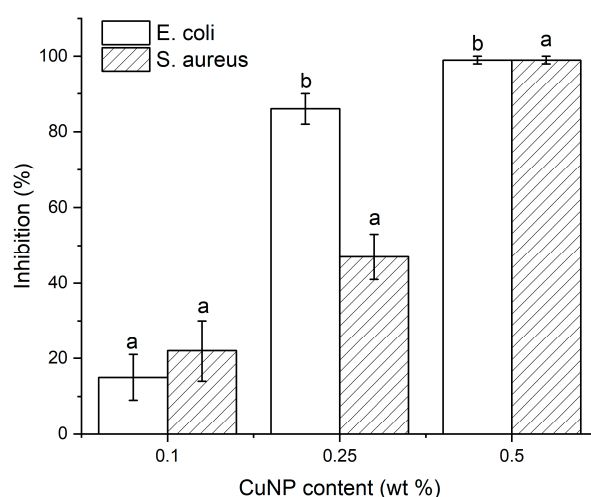


Figure 6. Inhibition (%) of core/shell multifilaments with different amounts of CuNP against *E. coli* and *S. aureus* strains. Different lowercase letters in the bars indicate a significant difference ($p \leq 0.05$).

Non-woven fabrics. On the other hand, for NWF samples with different CuNP content, the agar diffusion test was performed to identify their ability to inhibit the growth of pathogenic fungi and bacteria, see Figure 7. In the case of *C. albicans*, which causes oral candidiasis, is persistent in hospital environments, and can spread rapidly, no growth was observed in the area covered by the NWF sample, but only when using the highest content of CuNP 0.5% (*w/w*), and a similar behavior was presented for *S. aureus*. For *E. coli*, a total inhibition of bacterial growth was observed throughout the culture medium for all CuNP concentrations used. The above agrees with the results obtained in the tests for core/shell multifilaments, where *E. coli* showed greater susceptibility to CuNP from a concentration of 0.25% (*w/w*) with a content of 1.5×10^8 CFU/mL.

Although it was demonstrated that polymeric nanocomposites based on PET/CuNP have antimicrobial and antifungal activity, it is evident that more research is needed on the potential risks of these materials through the evaluation of cytotoxicity and other tests that demonstrate their safe use when in contact with human beings, in personal protective equipment, hospital textiles, filtration devices, etc. [29,30].

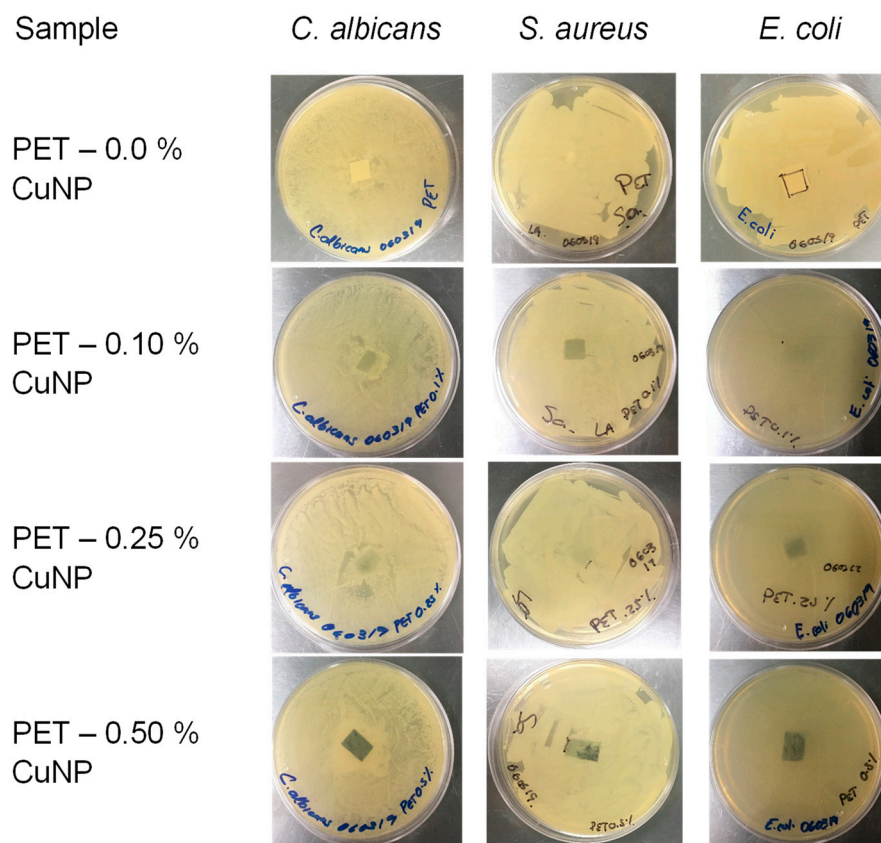


Figure 7. Agar diffusion tests for NWF samples with different CuNP content against *C. albicans*, *S. aureus*, and *E. coli*.

4. Discussion

Polyester fiber is the most important synthetic fiber in the world in terms of production due to its low cost, ease of processing, and excellent performance. Among its properties, polyester is a strong fiber (4.5 g/den) [25]. The growing demand to increase the properties of previously known fibers and to create new fields in the application of textile materials has caused the rapid growth of microfiber technology and the increasing potential of the textile industry [31].

Guerra et al. report the preparation of PET/Ag polymeric nanocomposites with different concentrations of Ag obtained by melt-mixing and subsequent dilution from a masterbatch [16]. During the thermal analysis of the nanocomposites obtained, they reported similar values for the T_g , T_c , and T_m of the polymer with and without adding Ag nanoparticles, similar to the results obtained in this study. However, the increase in the T_m of the 1% (*w/w*) PET/CuNP sample suggests that the Cu nanoparticles act as nucleation agents. Mata-Padilla et al. prepared polymer nanocomposites by ultrasound-assisted melt extrusion based on PP/Cu with different Cu contents. Through thermal analysis and particularly during non-isothermal crystallization at different rates, it was observed that the presence of CuNP promotes an increase in the rate and temperature of crystallization as the content of copper nanoparticles increases [32]. Other reports in the literature suggest that the main thermal transitions in polymeric nanocomposites are modified, particularly the crystallization and melting temperatures, due to the presence of metallic nanoparticles because these can promote the nucleation of polymeric crystals on their surface by acting as nucleation agents, even in very low concentrations < 5% (*w/w*) [33,34].

During the synthesis of PET and hybrids of PET-Ag/TiO₂ nanoparticles, degradation was observed in a single step and within the same temperature range for the pure polymer; meanwhile, the nanocomposite exhibited several weight loss events. The first occurring at a temperature of 253 °C equivalent to 9% by weight, and subsequently at 420 °C a loss of

84% by weight was observed and this is attributed to the thermal decomposition of PET derived from the byproducts present after the synthesis [35]. On the other hand, adding OMMT and/or SiO₂ at 0.5, 1, and 2% (*w/w*) in PET promotes a single degradation event in the same temperature interval as our sample [36].

Analysis of the dispersion of Cu in the nanocomposites and elemental analysis was performed using SEM in samples of LLDPE/Cu. The elemental analysis presents peaks associated with elemental copper and small traces of oxygen, suggesting partial oxidation of the particles upon contact with the environment [37].

The morphology of PP/CuO composites was analyzed by SEM. The size of the CuO particles was determined to be approximately less than 5 microns and the aggregation of CuO could have formed due to their high surface energy caused by the size effect of the particles. Furthermore, in a small amount, CuO is uniformly dispersed in PP matrix [27,33]. Zhou et al. showed similar results using SEM images of Cu₂O@ZrP hybrids on the surface of PET fibers, in addition to pointing out that melt-blending or in situ polymerization processes do not destroy the structure of Cu₂O@ZrP hybrids [13].

The addition of Cu₂O and Cu₂O@ZrP hybrids to a PET matrix and transformation in fibers using concentrations of 0.1, 0.2, 0.4, and 0.6% was performed by Zhou et al. and tested against *E. coli*, *S. aureus*, and *C. albicans*. Their results showed a microbial reduction of >99% for *E. coli* and *S. aureus*; meanwhile, *C. albicans* required a higher content of 0.6% to obtain a microbial decrease of 97% [13]. As expected, the design of the (textile) fiber has a significant influence on the inhibition of the growth of the microorganisms since, as shown previously, when the CuNP are confined to the outside of the filament (forming a shell with a high content of nanoparticles) the possibility of interaction with the cell wall of the microorganism increases and therefore can induce more significant damage, influencing the reproductive cycle. For its part, when the nanoparticles are dispersed throughout the cross-section of the filament, the possibility of interaction with the cell wall decreases; therefore, the antimicrobial properties also decrease at the same concentration. It has also been noted that the structure of the cell walls of Gram-positive and Gram-negative bacteria play an important role in susceptibility to various antimicrobial agents, with Gram-positive bacteria being more resistant than their Gram-negative counterparts [38,39].

Various reports in the literature have shown compelling evidence that metallic nanoparticles, their oxides, and alloys have antimicrobial activity and that this can be maintained when incorporated into a polymer matrix [6,7,31,38,40,41]. However, in the field of textiles, the addition of these nanoparticles has predominated at a stage subsequent to the manufacturing of the textile itself, mostly through impregnation methods [42,43]. Few reports in the literature have successfully tested the incorporation of nanoparticles in a polymeric matrix capable of being transformed into a textile and verifying that the antimicrobial activity is maintained [13–15].

The demand for functional textiles, particularly in the medical and healthcare sectors, requires the development of new materials that can efficiently satisfy these needs in an economical, safe, and sustainable manner. From previous results, two fundamental aspects are derived. The first indicates a close relationship between the size of the copper nanoparticles and their antibacterial properties because the probability of interaction with the cell wall of bacteria increases. This phenomenon occurs due to the adhesion of the fibers and CuNP exposed on the surface to the cell membrane of the *S. aureus* and *E. coli* strains in a way that damages the permeability and respiration of the bacteria. The inhibition in the growth/reproduction of bacteria is caused by the interaction of CuNP with sulfur-containing compounds, such as DNA, as proposed by [28,29,38]. The other aspect that is important to highlight is the design of the fiber itself [24] since by choosing a configuration of core (inert) and shell (active) the different concentrations of CuNP were confined in the shell of the filament, increasing the possibility of interaction with the cell wall of bacteria. The previous results could be very different if the entire cross-section of the filament contained the CuNP, since those found inside could not participate directly or come into direct contact with the cell wall of the bacteria, significantly reducing the inhibi-

tion of the growth of microorganisms, as shown in the NWF. To enhance the antimicrobial activity of NWF, two options arise: a change in fiber cross-section, for example, delta shape, or obtaining bi-component core/shell NWF [24,27].

5. Conclusions

By incorporating CuNP into a polyester resin, it was possible to modify its main thermal transitions, particularly the melting and crystallization temperature, without compromising its thermal stability. The above results suggest that the nanocomposite can be processed by melt-spinning and melt-blowing. Filaments with a core/shell configuration and NWF were obtained with concentrations of 0.1, 0.25, and 0.5% *w/w* CuNP. The denier and grammage increased as the nanoparticle content in the samples increased; nevertheless, only TD and DPF showed statistically significant differences. Through optical microscopy, it was possible to demonstrate a core/shell configuration formation.

On the other hand, the presence of CuNP was evident in the samples in both presentations, showing that the nanoparticles are homogeneously distributed and that some of them are exposed on the surface. Bacterial growth inhibition tests show that *E. coli* is more susceptible than *S. aureus*. When 0.5% CuNP is used in the core/shell multifilament, both bacteria exhibit an inhibition close to 100%, evidencing a bactericidal effect with a significant difference ($p \leq 0.05$). When an NWF is obtained, the inhibitory effect decreases significantly even against *C. albicans* and *S. aureus*; however, against *E. coli*, the samples have a high capacity to inhibit growth, even when using very low concentrations of CuNP. The design of the (textile) fiber has a significant influence on inhibiting the growth of the microorganism since if the antimicrobial additive is confined to a surface layer of the fiber (core/shell multifilaments) instead of dispersing throughout the cross-section of the fiber (NWF), the antimicrobial effect is increased.

6. Patents

Patent (granted) MX 385261—2021.

Author Contributions: Conceptualization, C.A.Á.-O. and V.J.C.-D.; methodology, F.S.-C. and A.S.L.-P.; validation, F.S.-C., A.S.L.-P. and N.R.-F.; formal analysis, A.G.-S. and F.S.-C.; investigation, R.R.-M. and J.E.H.-B.; resources, J.A.V.-G.; writing—original draft preparation, A.G.-S., R.R.-M. and J.E.H.-B.; writing—review and editing, C.A.Á.-O. and V.J.C.-D.; visualization, F.S.-C.; supervision, F.S.-C., A.S.L.-P. and N.R.-F.; project administration, J.A.V.-G. and V.J.C.-D.; funding acquisition, C.A.Á.-O. All authors have read and agreed to the published version of the manuscript.

Funding: This research was supported by Innovate UK/CONACYT/Newton Fund, “Antimicrobial Textiles for the Health Sector” (ACTin), Grants: 268003 (MX) and 102729 (UK). Thanks to the National Council of Humanities, Science and Technology (CONAHCyT) for the scholarship awarded (A.G.-S.).

Data Availability Statement: Data are contained within the article.

Acknowledgments: Thanks to Maria Guadalupe Mendez, Alfonso Mercado, Carmen Alvarado, and Martha Alicia Fernandez for their technical support.

Conflicts of Interest: The authors declare no conflicts of interest. The patent ownership is granted by the Research Center for Applied Chemistry (CIQA); the inventors involved are J.A.V.G., F.S.C., C.A.A.O. and V.J.C.D. The funders had no role in the design of the study; in the collection, analyses, or interpretation of data; in the writing of the manuscript; or in the decision to publish the results.

References

1. Forrester, J.D.; Maggio, P.M.; Tennakoon, L. Cost of Health Care—Associated Infections in the United States. *J. Patient Saf.* **2022**, *18*, e477–e479. [[CrossRef](#)] [[PubMed](#)]
2. Wilcox, M.H.; Dryden, M. Update on the Epidemiology of Healthcare-Acquired Bacterial Infections: Focus on Complicated Skin and Skin Structure Infections. *J. Antimicrob. Chemother.* **2021**, *76*, iv2–iv8. [[CrossRef](#)] [[PubMed](#)]
3. Zimlichman, E.; Henderson, D.; Tamir, O.; Franz, C.; Song, P.; Yamin, C.K.; Keohane, C.; Denham, C.R.; Bates, D.W. Health Care-Associated Infections: A Meta-Analysis of Costs and Financial Impact on the US Health Care System. *JAMA Intern. Med.* **2013**, *173*, 2039–2046. [[CrossRef](#)] [[PubMed](#)]

4. Tanasa, F.; Teaca, C.-A.; Nechifor, M.; Ignat, M.; Duceac, I.A.; Ignat, L. Highly Specialized Textiles with Antimicrobial Functionality—Advances and Challenges. *Textiles* **2023**, *3*, 219–245. [[CrossRef](#)]
5. Gulati, R.; Sharma, S.; Sharma, R.K. Antimicrobial Textile: Recent Developments and Functional Perspective. *Polym. Bull.* **2022**, *79*, 5747–5771. [[CrossRef](#)] [[PubMed](#)]
6. Bashari, A.; Shakeri, M.; Shirvan, A.R.; Najafabadi, S.A.N. Functional Finishing of Textiles via Nanomaterials. In *Nanomaterials in the Wet Processing of Textiles*; Wiley-Scrivener: Austin, TX, USA, 2018; pp. 1–70, ISBN 9781119459804.
7. Sowa-Söhle, E.N.; Schwenke, A.; Sajti, C.L.; Wagener, P.; Weiss, A.; Wiegel, H.; Haverich, A. Antimicrobial Efficacy, Cytotoxicity, and Ion Release of Mixed Metal (Ag, Cu, Zn, Mg) Nanoparticle Polymer Composite Implant Material. *BioNanoMaterials* **2013**, *14*, 217–227. [[CrossRef](#)]
8. Vu, N.N.; Venne, C.; Ladhari, S.; Saidi, A.; Moskovchenko, L.; Lai, T.T.; Xiao, Y.; Barnabe, S.; Barbeau, B.; Nguyen-Tri, P. Rapid Assessment of Biological Activity of Ag-Based Antiviral Coatings for the Treatment of Textile Fabrics Used in Protective Equipment against Coronavirus. *ACS Appl. Bio Mater.* **2022**, *5*, 3405–3417. [[CrossRef](#)] [[PubMed](#)]
9. Parham, S.; Kharazi, A.Z.; Bakhsheshi-Rad, H.R.; Kharaziha, M.; Ismail, A.F.; Sharif, S.; Razzaghi, M.; RamaKrishna, S.; Berto, F. Antimicrobial Synthetic and Natural Polymeric Nanofibers as Wound Dressing: A Review. *Adv. Eng. Mater.* **2022**, *24*, 2101460. [[CrossRef](#)]
10. Su, X.; Sha, Q.; Gao, X.; Li, J.; Wu, Y.; Li, W.; Wu, W.; Han, N.; Zhang, X. Lightweight, Multifunctional Smart MXene@PET Non-Woven with Electric/Photothermal Conversion, Antibacterial and Flame Retardant Properties. *Appl. Surf. Sci.* **2023**, *639*, 158205. [[CrossRef](#)]
11. Saylor, Y.; Irby, V. *Metal Nanoparticles: Properties, Synthesis and Applications*; Nova Science Publishers: Hauppauge, NY, USA, 2018; ISBN 9781536141160.
12. Ren, G.; Hu, D.; Cheng, E.W.C.; Vargas-Reus, M.A.; Reip, P.; Allaker, R.P. Characterisation of Copper Oxide Nanoparticles for Antimicrobial Applications. *Int. J. Antimicrob. Agents* **2009**, *33*, 587–590. [[CrossRef](#)]
13. Zhou, J.; Fei, X.; Li, C.; Yu, S.; Hu, Z.; Xiang, H.; Sun, B.; Zhu, M. Integrating Nano-Cu₂O@ZrP into in Situ Polymerized Polyethylene Terephthalate (PET) Fibers with Enhanced Mechanical Properties and Antibacterial Activities. *Polymers* **2019**, *11*, 113. [[CrossRef](#)]
14. Zhu, Y.; Wang, Y.; Sha, L.; Zhao, J. Preparation of Antimicrobial Fabric Using Magnesium-Based PET Masterbatch. *Appl. Surf. Sci.* **2017**, *425*, 1101–1110. [[CrossRef](#)]
15. Yeo, S.Y.; Jeong, S.H. Preparation and Characterization of Polypropylene/Silver Nanocomposite Fibers. *Polym. Int.* **2003**, *52*, 1053–1057. [[CrossRef](#)]
16. Guerra, M.A.; Mariano, N.A.; Ramos, A.S.; Campos, M.G.N. Processing of Pet-Silver Nanocomposite Filaments. *Mater. Sci. Forum* **2016**, *869*, 350–355. [[CrossRef](#)]
17. Guzman, A.; Cárcamo, H.; León, O. Elaboración y Caracterización Estructural de Fibras de Tereftalato de Polietileno (PET) Dopadas Con Nanocobre (0) Utilizando Proceso de Extrusión. *Rev. Peru. Química e Ing. Química* **2014**, *17*, 9–13.
18. Abazari, M.; Badeleh, S.M.; Khaleghi, F.; Saeedi, M.; Haghi, F. Fabrication of Silver Nanoparticles-Deposited Fabrics as a Potential Candidate for the Development of Reusable Facemasks and Evaluation of Their Performance. *Sci. Rep.* **2023**, *13*, 1593. [[CrossRef](#)] [[PubMed](#)]
19. Ferreira, T.; Vale, A.C.; Pinto, A.C.; Costa, R.V.; Pais, V.; Sousa, D.; Gomes, F.; Pinto, G.; Dias, J.G.; Moreira, I.P.; et al. Comparison of Zinc Oxide Nanoparticle Integration into Non-Woven Fabrics Using Different Functionalisation Methods for Prospective Application as Active Facemasks. *Polymers* **2023**, *15*, 3499. [[CrossRef](#)] [[PubMed](#)]
20. Chruściel, J.J.; Olczyk, J.; Kudzin, M.H.; Kaczmarek, P.; Król, P.; Tarzyńska, N. Antibacterial and Antifungal Properties of Polyester, Polylactide, and Cotton Nonwovens and Fabrics, by Means of Stable Aqueous Dispersions Containing Copper Silicate and Some Metal Oxides. *Materials* **2023**, *16*, 5647. [[CrossRef](#)] [[PubMed](#)]
21. Gabbay, J.; Borkow, G.; Mishal, J.; Magen, E.; Zatzoff, R.; Shemer-Avni, Y. Copper Oxide Impregnated Textiles with Potent Biocidal Activities. *J. Ind. Text.* **2006**, *35*, 323–335. [[CrossRef](#)]
22. Ávila-Orta, C.A.; Quiñones-Jurado, Z.V.; Waldo-Mendoza, M.A.; Rivera-Paz, E.A.; Cruz-Delgado, V.J.; Mata-Padilla, J.M.; González-Morones, P.; Ziolo, R.F. Ultrasound-Assist Extrusion Methods for the Fabrication of Polymer Nanocomposites Based on Polypropylene/Multi-Wall Carbon Nanotubes. *Materials* **2015**, *8*, 7900–7912. [[CrossRef](#)]
23. *JIS Z 2801*; Antibacterial Products—Test for Antibacterial Activity and Efficacy. Japanese Standards Association: Tokyo, Japan, 2010.
24. Naeimirad, M.; Zadhoush, A.; Kotek, R.; Esmaeely Neisiany, R.; Nouri Khorasani, S.; Ramakrishna, S. Recent Advances in Core/Shell Bicomponent Fibers and Nanofibers: A Review. *J. Appl. Polym. Sci.* **2018**, *135*, 46265. [[CrossRef](#)]
25. Karaca, E.; Ozcelik, F. Influence of the Cross-Sectional Shape on the Structure and Properties of Polyester Fibers. *J. Appl. Polym. Sci.* **2007**, *103*, 2615–2621. [[CrossRef](#)]
26. Lim, J.C.; Park, Y.W.; Kim, H.C. Study on Manufacturing PCT/PPS Flame Retardant Fiber by Sheath/Core Conjugate Spinning. *Fibers Polym.* **2020**, *21*, 498–504. [[CrossRef](#)]
27. Kara, S.; Ureyen, M.E.; Erdogan, U.H. Structural and Antibacterial Properties of PP/CuO Composite Filaments Having Different Cross Sectional Shapes. *Int. Polym. Process.* **2016**, *31*, 398–409. [[CrossRef](#)]

28. España-Sánchez, B.L.; Ávila-Orta, C.A.; Padilla-Vaca, F.; Neira-Velázquez, M.G.; González-Morones, P.; Rodríguez-González, J.A.; Hernández-Hernández, E.; Rangel-Serrano, Á.; Barriga Castro, E.D.; Yate, L.; et al. Enhanced Antibacterial Activity of Melt Processed Poly(Propylene) Ag and Cu Nanocomposites by Argon Plasma Treatment. *Plasma Process. Polym.* **2014**, *11*, 353–365. [[CrossRef](#)]
29. Tamayo, L.; Azócar, M.; Kogan, M.; Riveros, A.; Páez, M. Copper-Polymer Nanocomposites: An Excellent and Cost-Effective Biocide for Use on Antibacterial Surfaces. *Mater. Sci. Eng. C* **2016**, *69*, 1391–1409. [[CrossRef](#)] [[PubMed](#)]
30. García, A.; Rodríguez, B.; Giraldo, H.; Quintero, Y.; Quezada, R.; Hassan, N.; Estay, H. Copper-Modified Polymeric Membranes for Water Treatment: A Comprehensive Review. *Membranes* **2021**, *11*, 93. [[CrossRef](#)]
31. Peng, N.; Widjojo, N.; Sukitpaneelit, P.; Teoh, M.M.; Lipscomb, G.G.; Chung, T.-S.; Lai, J.-Y. Evolution of Polymeric Hollow Fibers as Sustainable Technologies: Past, Present, and Future. *Prog. Polym. Sci.* **2012**, *37*, 1401–1424. [[CrossRef](#)]
32. Mata-Padilla, J.M.; Ávila-Orta, C.A.; Almendárez-Camarillo, A.; Martínez-Colunga, J.G.; Hernández-Hernández, E.; Cruz-Delgado, V.J.; González-Morones, P.; Solís-Rosales, S.G.; González-Calderón, J.A. Non-Isothermal Crystallization Behavior of Isotactic Polypropylene/Copper Nanocomposites. *J. Therm. Anal. Calorim.* **2020**, *143*, 2919–2932. [[CrossRef](#)]
33. Tamayo, L.; Palza, H.; Bejarano, J.; Zapata, P.A. Polymer Composites with Metal Nanoparticles: Synthesis, Properties, and Applications. In *Polymer Composites with Functionalized Nanoparticles: Synthesis, Properties, and Applications*; Elsevier: Amsterdam, The Netherlands, 2018; pp. 249–286, ISBN 9780128140659.
34. Demchenko, V.; Riabov, S.; Rybalchenko, N.; Shtompel', V. Structure, Morphology, and Properties of Copper-Containing Polymer Nanocomposites. In *Nanophysics, Nanomaterials, Interface Studies, and Applications, Proceedings of the 4th International Conference Nanotechnology and Nanomaterials (NANO2016), Lviv, Ukraine, 24–27 August 2016*; Springer: Cham, Switzerland, 2017; Volume 195, pp. 641–659.
35. De León-Martínez, P.A.; Soriano-Corral, F.; Ávila-Orta, C.A.; González-Morones, P.; Hernández-Hernández, E.; Ledezma-Pérez, A.S.; Covarrubias-Gordillo, C.A.; Espinosa-López, A.C.; de León Gómez, R.E.D. Surface Modification of NTiO₂/Ag Hybrid Nanoparticles Using Microwave-Assisted Polymerization in the Presence of Bis(2-Hydroxyethyl) Terephthalate. *J. Nanomater.* **2017**, *2017*, 7079497. [[CrossRef](#)]
36. Vassiliou, A.A.; Chrissafis, K.; Bikiaris, D.N. In Situ Prepared PET Nanocomposites: Effect of Organically Modified Montmorillonite and Fumed Silica Nanoparticles on PET Physical Properties and Thermal Degradation Kinetics. *Thermochim. Acta* **2010**, *500*, 21–29. [[CrossRef](#)]
37. Xue, B.; Jiang, Y.; Liu, D. Preparation and Characterization of a Novel Anticorrosion Material: Cu/LLDPE Nanocomposites. *Mater. Trans.* **2011**, *52*, 96–101. [[CrossRef](#)]
38. España-Sánchez, B.L.; Ávila-Orta, C.A.; Padilla-Vaca, L.F.; Barriga-Castro, E.D.; Soriano-Corral, F.; González-Morones, P.; Ramírez-Wong, D.G.; Luna-Barcenas, G. Early Stages of Antibacterial Damage of Metallic Nanoparticles by TEM and STEM-HAADF. *Curr. Nanosci.* **2017**, *14*, 54–61. [[CrossRef](#)]
39. Pardi, G. “Determinantes de Patogenicidad de Candida Albicans”: (Revisión Bibliográfica). *Acta Odontol. Venez* **2002**, *40*, 185–192.
40. Dong, X.; Wang, S.; Ren, K. Application of Composite Antibacterial Nanoparticle Non-Woven Fabric in Sterilization of Hospital Infection. *Prev. Med.* **2023**, *173*, 107597. [[CrossRef](#)]
41. Fernandez, A.; Lloret, E.; Llorens, A.; Picouet, P. Metal-Based Micro and Nano-Composites as Antimicrobials in Food Packaging. In *Food Packaging: Procedures, Management and Trends*; Nova Science Publishers: Hauppauge, NY, USA, 2012; pp. 79–92, ISBN 9781622573103.
42. Ghosh, S.; Sarkar, B.; Thongmee, S.; Mostafavi, E. Hybrid Antibacterial, Antifungal, and Antiviral Smart Coatings. In *Antiviral and Antimicrobial Smart Coatings: Fundamentals and Applications*; Elsevier: Amsterdam, The Netherlands, 2023; pp. 431–452, ISBN 9780323992916.
43. Odintsova, O.I.; Vladimirtseva, E.L.; Kozlova, O.V.; Smirnova, S.V.; Lipina, A.A.; Petrova, L.S.; Erzunov, K.A.; Konstantinova, Z.A.; Zimnurov, A.R.; Bykov, F.A.; et al. Finishing textile materials with microcapsules and nanoparticles of functional substances. *ChemChemTech* **2023**, *66*, 173–184. [[CrossRef](#)]

Disclaimer/Publisher’s Note: The statements, opinions and data contained in all publications are solely those of the individual author(s) and contributor(s) and not of MDPI and/or the editor(s). MDPI and/or the editor(s) disclaim responsibility for any injury to people or property resulting from any ideas, methods, instructions or products referred to in the content.